Preprint Cambridge Centre for Computational Chemical Engineering ISSN 1473 – 4273

Size spectra and source apportionment of fine particulates in tropical urban environment during southwest monsoon season

Yichen Zong[1], Maria L. Botero[1], Liya E. Yu[2], Markus Kraft[3,4]

released: June 21, 2018

[1] Department of Mechanical Engineering
National University of Singapore
9 Engineering Drive
117575, Singapore

[2] Department of Civil and Environmental Engineering
National University of Singapore
1 Engineering Drive
117576, Singapore

[3] School of Chemical and Biomedical Engineering
Nanyang Technological University
62 Nanyang Drive
637459, Singapore

[4] Department of Chemical Engineering and Biotechnology
University of Cambridge
West Cambridge Site
Philippa Fawcett Drive
Cambridge CB3 0AS
United Kingdom
E-mail: mk306@cam.ac.uk

Preprint No. 201

Keywords: PM emission, source apportionment, PMF, Southeast Asia

Edited by
Computational Modelling Group
Department of Chemical Engineering and Biotechnology
University of Cambridge
West Cambridge Site
Philippa Fawcett Drive
Cambridge CB3 0AS
United Kingdom

Fax: + 44 (0)1223 334796
E-Mail: c4e@cam.ac.uk
World Wide Web: http://como.cheng.cam.ac.uk/

Abstract

In this study, we carried out high time-resolution measurements of particle number concentration and size distribution (5-1000 nm) in Singapore, which represents a tropical urban environment. The measurements were taken during the southwest monsoon season in 2017 using a fast-response differential mobility spectrometer at a sampling rate of 1 Hz. In the measurement, short-lived nucleation events were found prominent at early afternoon because of the abundant incoming radiation that enhances the photochemical reactions in atmosphere. For the first time in the region, a five-factor positive matrix factorization approach was applied to the size spectra data. Based on PM number concentration, two sources within nucleation mode (<30 nm) were resolved and account for 43.5% of total number concentration, which is higher than the available monitoring data in other big cities. Among the sources, O_3-related atmospheric photochemical reactions with peak size at 10-12 nm is a unique factor and prominent in early afternoon nucleation events. The findings of this work can serve as a baseline for assessing influence of local and cross-border airborne PM emissions during various seasons in the future.

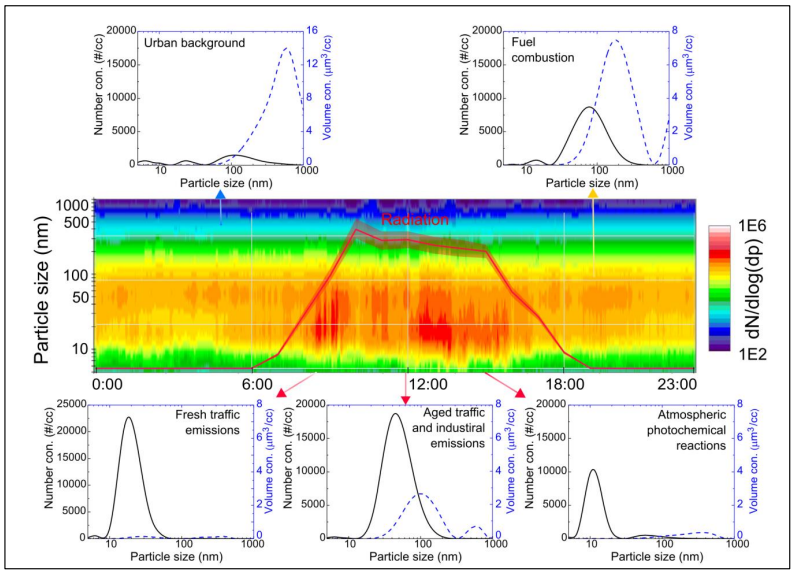

Highlights:

- Full size spectra of airborne fine particulates were measurement at high frequency (1Hz) in Singapore, representing a tropical urban environment.
- Significant nucleation events were observed at early afternoon during southwest monsoon season.
- Source apportionment on particle size spectra data was performed for the first time in Southeast Asia.
- A unique source was discovered within nucleation mode that correlates with O_3-related atmospheric photochemical reactions.

1 Introduction

Air pollution is a major urban problem and presents a big challenge for the sustainable development of modern cities. Long-term exposure to ambient Particulate Matter (PM) is associated with increased mortality and morbidity from cardiovascular and pulmonary diseases [1, 2]. Epidemiological studies have also demonstrated that ultrafine particles (UFP, <100 nm) from PM may have sever adverse health effects, considering their larger likelihood of penetration and higher surface area per unit volume to adsorb organic compounds [3, 4].

Currently, air quality is measured and controlled in mass concentration as the standard metric. However, these metric does not consider the spectra of particle sizes, specifically the contribution of ultrafine particles. Ultrafine particles are negligible in mass but comprise the major proportion (80%) in total number concentration from ambient PM measurement [5]. Thus, in order to generate relevant and reasonable regulations, it is important to understand the size distribution and number concentration of ultrafine particles in the air, as well understanding the extent to which different emitters contribute to these particles.

Tropical urban regions in Southeast Asia are reported to have serious air pollution issues from airborne PM emissions in recent years [6–8], while relevant studies remain sparse. For these densely populated cities, particulate matter is emitted from a diverse mixture of mobile sources (air, ground and marine transportation) and stationary (industrial) sources. In Singapore, for example, five major sources were identified in 2001 as solid dust, metallurgical industry, biomass fires/local traffic, sea-salt and oil combustion, from a principal component analysis on chemical species data [9]. Later studies attribute the burning of biomass (in bush fires) in Sumatra as a major source of local airborne PM emissions [10, 11]. A typical report on 2013 haze event shows that particles larger than 0.2 mm in diameter is remarkably higher than on normal days [12]. Besides, traffic-related emissions and the exposure to daily commuting have also been studied [13, 14], the gasoline-powered vehicles are found to make a higher contribution to aerosol components than the diesel-powered vehicles [15]. From these most recent literature, the contribution of bush fires is no longer the most concerning source in Singapore in recent years and a new and comprehensive re-assessment of the sources of airborne PM emissions is needed, which can work as a baseline for studies and regulations on local air quality.

Another significant factor contributing ultrafine particles in modern cities is the nucleation event, which occurs in both clean and polluted environments by homogeneous nucleation or heterogamous nucleation [16]. Strong nucleation events are usually observed at high temperature, solar radiation, low relative humidity (RH) and low-condensation sink conditions [17, 18]. It has been suggested that the nucleation events could be caused by local precursors from traffic, ship or aircraft emissions [19].

Positive Matrix Factorization (PMF) is an established method developed by Paatero [20, 21] that has previously been used to apportion the sources of airborne PM emissions by analyzing the chemical composition of the samples [22–24]. Recently, the method was also found effective on particle number concentration and size distribution (PNSD) data [25, 26], which has received much attention with a rapid increase in publications.

The method is based on the assumption that different sources will produce characteristic size distributions, just like fingerprints. The measured particle size distribution can then be described as a sum of characteristic size distributions from different sources. Up to now, the PMF analysis on particle size distribution has been performed in major cities in the world, including London, New York city and Beijing. A list of PNSD source profiles from those studies has been reviewed in detail [27].

This study aims to investigate the possible sources of airborne PM emissions in Singapore during the southwest monsoon in 2017, which represents a typical tropical urban environment in Southeast Asia. This period is of particular interest because it represents a season without major external pollution sources, and the resulting PM characteristics and sources can thus be considered as a baseline for Singapore emissions. In this research, the particle size distribution between 5 nm-100 nm was measured at 1 Hz using a fast particle analyzer (DMS500). For the first time in the region, real-time PNSD spectra were measured and used to perform the source apportionment by PMF with combined meteorological data and bivariate conditional probability function (CPF) analysis. The major five source profiles and their contributions were determined and quantified.

2 Experimental methodology

2.1 On-site sampling

The sampling campaign was carried out during the 2017 southwest monsoon season in Singapore from 31 July to 8 October (36 days). The site was selected at the open terrace at the third floor of a building ($1^{\circ}18'13.8''$N, $103^{\circ}46'25.76''$E), which is shown in the map in Fig. 1. The Clementi road is 50 m away from the sampling site in the west, and the AYE Expressway is 30 m away from the sampling site in the south. Clementi road is an arterial road from north to south and AYE Expressway is the major link of east and west Singapore and has a busy traffic all day long. As one of the busiest harbors in the world, it is estimated that about 3300 ships transect Singapore strait per day [17]. The closest harbor (Pasir Panjang terminal) is located at 2 km away in the south. A large industrial park is located 6 km away in the southwest (only a small part shown in the map). The industrial park is specialized for the petrochemical industry. The industrial park is specialized for the petrochemical industry. In addition, a power plant is located at about 26 km in the west and another one at about 20 km in the northeast of the site (not shown in the figure). They could play a role in cross-border emissions considering the limited land area of Singapore.

A DMS500 (Cambustion Ltd., Cambridge) fast-response differential mobility spectrometer was used in this study. DMS has been widely used in both engine emission studies and environment measurement, detailed description of DMS can be found in previous studies [28–30]. It is capable of measuring particle number contribution and size distribution (PNSD) from 5-1000 nm at a maximum frequency of 10 Hz. In this study, the measurement was recorded at 1 Hz to improve the signal/noise ratio. The fast response time (1s) of DMS can provide a real-time measurement of airborne PM emissions. The meteorological conditions were recorded at the NUS Geography weather station every

5 min, including atmospheric pressure, air temperature, relative humidity, rainfall, solar irradiance, wind speed and wind direction (*inetapps.nus.edu.sg/fas/geog*). The station is at a distance of 700 m to south from the sampling site and at a height of about 67 m above sea level. Pollutant mass concentrations of $PM_{10}, PM_{2.5}, O_3, NO_2, SO_2$ and CO are provided by Singapore National Environment Agency (NEA) from the South monitoring station (*data.gov.sg/group/environment*).

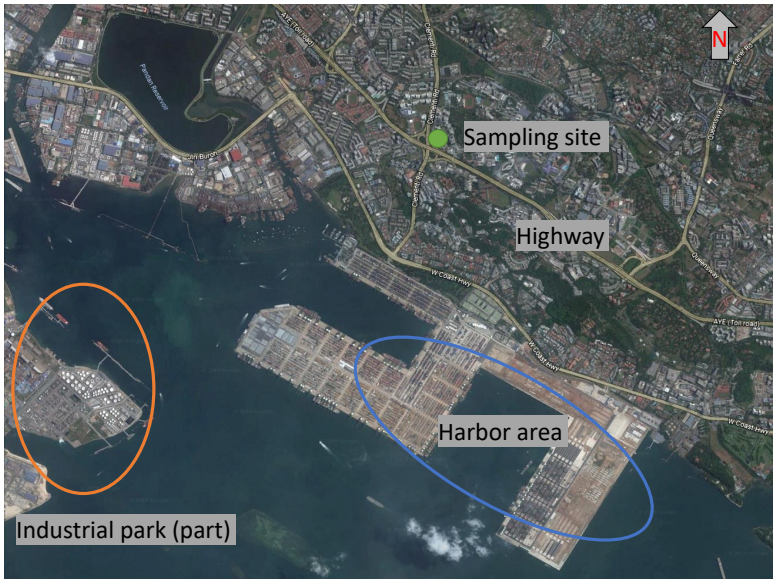

Figure 1: *Map of studied area.*

2.2 Data processing

Data were collected and managed by MongoDB 3.4, which is an open-source database tool widely used in statistics and scientific research. In total, 3,272,112 valid PNSD spectra were stored in the database, along with meteorological information recorded during the measurement campaign. Data analysis was performed in Matlab R2016B and R 3.4.3, using the Openair package [31].

PMF analysis was performed by using the US EPA PMF5 [32], this latest version incorporates three error estimation (EE) methods for analyzing factor solutions, i.e., classical bootstrap (BS), displacement of factor elements (DISP) and bootstrap enhanced by displacement (BS-DISP). Mathematically, PMF is a tool that decomposes a large matrix (i.e., measured data) into two smaller non-negative matrices (i.e., factor contributions and factor profiles). For the observation matrix X,

$$x_{ij} = \sum_{k=1}^{p} g_{ik} f_{kj} + e_{ij} \tag{1}$$

where g_{ik} represents the contributions of factor k to sample i; f_{kj} depicts the factor profiles of factor k in size bin j; e_{ij} is the residual for sample i in the size bin j. PMF solves the

problem by minimizing the sum of weighted least squares, Q:

$$\{g, f\} = \arg\min_{g,f} Q \tag{2}$$

with

$$Q = \sum_{i=1}^{m} \sum_{j=1}^{n} \left(\frac{e_{ij}}{u_{ij}} \right)^2 \tag{3}$$

where u_{ij} represents measurement uncertainties. The uncertainties of DMS data were estimated from the method detection limit (MDL) [32], which is provided by the instrument manufacturer (Cambustion Ltd., Cambridge)

$$u_{ij} = \begin{cases} \frac{5}{6}\text{MDL}, & x_{ij} \leq \text{MDL} \\ \sqrt{(\varepsilon x_{ij})^2 + (0.5\text{MDL})^2}, & x_{ij} > \text{MDL} \end{cases} \tag{4}$$

where the error fraction ε was determined by a trial and error approach from 5%-15% [30, 33]. An optimization of ε was carefully conducted based on the EPA manual and literature reports [34, 35], i.e., (1) Reducing the number of size bins with low signal-to-noise (S/N) ratios; (2) Reducing the number of size bins with large absolute scaled residuals (a threshold of 3 was used); (3) the best calculated value for Q with respect to the expected value calculated as suggested by [36]; In this case, best PMF outputs were found when $\varepsilon = 10\%$.

The choice of the number of factors is a compromise between too many factors that may split a real source into multiple none-existing sources, and too few factors that may combine different real sources. In this work, the best solutions were selected from testing from 4 to 9 factors under the guideline of EPA manual and literature reports [34, 35], i.e., (1) Evaluating the possible pollutant sources in Singapore and their impacts; (2) Obtaining convergence and stable Q over all the runs; (3) Obtaining a good fitting for total particle number concentration ($R^2 > 0.9, \text{slope} \rightarrow 1$); (4) Reducing the number of samples with large absolute scaled residual (a threshold of 3 was used); (5) the best calculated value for Q with respect to the expected value [36]; (6) Adopting the statistics tools provided by the software (DISP, BS and BS-DISP).

Bivariate conditional probability function (CPF) analysis was adopted to analyze the impacts of wind on source apportionment results [37]. The CPF is defined as,

$$P(C \geq C_0 \mid \triangle\theta, \triangle v) = \frac{m_{C \geq C_0, \triangle\theta, \triangle v}}{n_{\triangle\theta, \triangle v}} \tag{5}$$

where m is the number of samples in the wind sector $\triangle\theta$ with wind speed interval $\triangle v$ having number concentration C no less than a threshold value C_0, and n is the total number of samples in the same wind direction-speed interval $\triangle\theta, \triangle v$. The threshold criterion was set at 75th percentile considering the sample size in this study.

3 Results and Discussion

3.1 Diurnal and nocturnal patterns

In Singapore, the typically tropical climate features for high temperature and high humidity. During the measurement campaign, the recorded mean temperature is 27.4±1.6°C and the mean relative humidity (RH) is 77.0±9.4%. The southwest monsoon is one of the two major monsoon seasons in Singapore and generally prevails from June to early October. The wind rose diagram for the measurement period is shown in Fig. 2. The mean wind speed is 1.8±1.6 m/s, which can be categorized as calm to light breeze. The winds are mostly from the south, developed over the island of Sumatra in the south or Straits of Malacca in the west. In the studied area, the diurnal pattern of the weather is much more prominent, due to the strong influence of solar radiation in tropical area [17]. As shown in Fig. 3a, temperature starts to increase from 26.3°C in the morning as the sun rises, and reaches a peak at 28.7°C at 13:00 hrs, then it decreases till the next morning. The lowest temperature of a day is generally between 6:00-7:00 hrs just before the sunrise. The variation of humidity shows the opposite pattern to the temperature. Generally, at 7:00 hrs in the morning RH reaches a peak at 81.4%, it then decreases to the lowest point of a day at 69.6% as temperature rises. At nighttime (19:00-6:00 hrs), RH remains higher than 75.0% and increases till the next morning. The diurnal pattern of incoming radiation is presented in Fig. 3b, showing that radiation is abundant in Singapore and remains high from 10:00-15:00 hrs above 300 W/m^2. The incoming radiation is the driving force for the rise of temperature and the drop of RH during daytime (7:00-18:00 hrs).

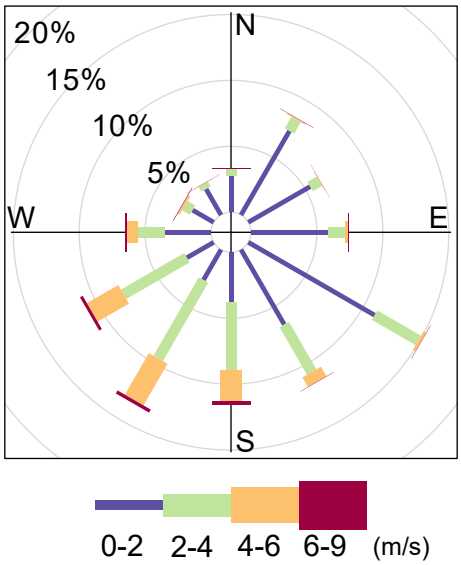

Figure 2: *Wind rose diagram during the southwest monsoon.*

The diurnal and nocturnal pattern of PNSD spectra (5 nm-1000 nm) is presented in Fig. 3b. The plot corresponds to an average of the daily spectra obtained during the measurement campaign. It is observed that 90.2% of the particles in number concentration is attributed to ultrafine particles (<100 nm) in this study, which is consistent with the observation in

other big cities across the world [38]. During daytime, from 8:00-15:00 hrs, ultrafine particles significantly emerge, which can be due to both primary emissions and secondary formation, such as traffic and gas-to-particle conversion (GTP) [17, 19]. The latter could indicate the occurrence of nucleation events, also called new particle formation (NPF) events [39, 40]. The nucleation events are favored by high radiation conditions, because they are driven by photochemical reactions in the atmosphere [27]. In Fig. 3b, the emerging of ultrafine particles also coincides with the time when incoming radiation is prominent, temperature is high and RH is low. Interestingly, no further size growth can be seen for these ultrafine particles in the spectra, which can indicate that these nucleation events could be short-lived [19, 39]. During these short-lived nucleation events, the existing large particles in submicron and micron ranges, which are named condensation sinks (CS), can absorb the precursor gases and suppress the small particle growth. In Singapore, CS is reported to be higher than most of the studies from other parts of the world [17]. Similar short-lived nucleation events have been also reported in Brisbane, Australia, in a subtropical urban environment [40].

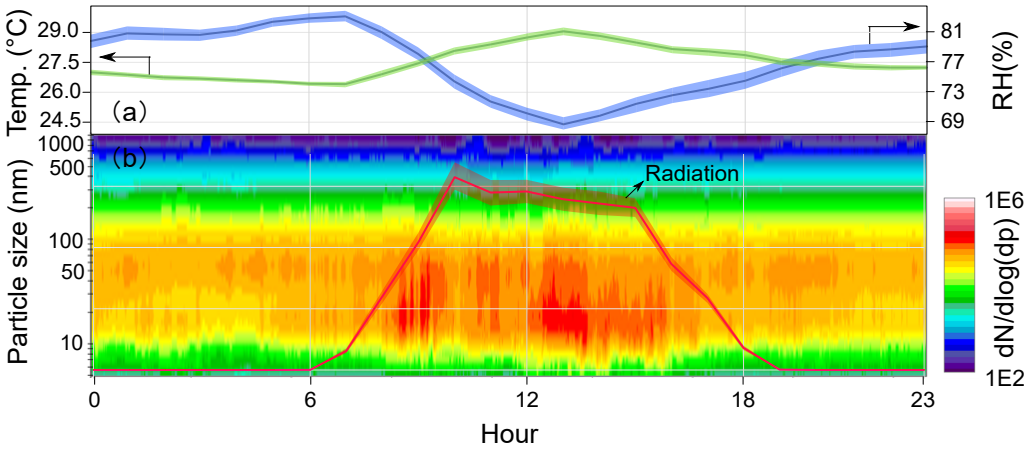

Figure 3: *Top: hourly pattern of temperature and relative humidity; Bottom: contour of of PNSD and the hourly pattern of incoming radiation. The shaded area represents the 95% confidence interval.*

For a more detailed analysis, the measured particle size distribution can be divided into three regions, i.e., nucleation mode (5-30 nm), Aitken mode (30-100 nm) and accumulation mode (100-1000 nm) [27]. Such classification is useful for an identification of the possible sources of airborne PM emissions, prior to a source apportionment study. Fig. 4a presents the time evolution of the number concentration of particles in the different modes (all the concentrations are above instrument sensitivity). The daily total number concentration is dominated (>85%) by nucleation and Aitken mode particles that are smaller than 100 nm. The contribution of accumulation mode particles on total number concentration is negligible, although they dominate (>90%) the volume based concentration as observed in Fig. 4b. Here the diurnal and nocturnal pattern for volume concentration is calculated assuming that the particles are all spherical. Temporal trend in mass concentrations of PM_{10}, $PM_{2.5}$, O_3, NO_2, SO_2 and CO are plotted in **Fig. S1** for complementary analysis of trend based on the mean data provided by NEA for certain pollutants.

Three major peaks are observed from the diurnal and nocturnal pattern of total number

concentration. The first one at 9:00 hrs has a peak value of 3.67×10^4 #/cc, comprising a combined contribution from the Aitken mode and nucleation mode particles, with a slightly larger contribution from the former. The peak occurs during morning traffic rush hours, which entails that the high concentration of nucleation and Aitken mode particles could result from the traffic emissions. This peak is supported by the concurrent peak at 9:00 hrs in hourly CO concentration in **Fig. S1**. The second peak falls between 12:00-15:00 hrs with the highest value of 3.98×10^4 #/cc. Overall, the early afternoon peak is dominated by the nucleation mode particles. The sharp peak demonstrates a rapid increase in the number of particles that can be attributed mainly to abundant incoming radiation, highest temperature and lowest RH of the day shown in Fig. 3b. Considering the sparse traffic at that time, these nucleation mode particles should be formed in the atmosphere mainly via secondary processes of photooxidation converting gas to particles. The formation of these secondary aerosols is substantiated by the concurrently increasing concentration of O_3 in **Fig. S1**, demonstrating prominent atmospheric photooxidation. The last peak occurs at 20:00 hrs with a concentration of 2.71×10^4 #/cc. This peak also coincides with increasing concentrations in both CO and NO_2 in **Fig. S1**, suggesting emissions of combustion processes.

In contrast to the number concentration, the volume concentration has far less variation and remains at 12-16 μm^3/cc. This is expected since total volume concentration of airborne PM emissions is mainly contributed by larger particles, or accumulation mode particles. A low point of total volume concentration (12 μm^3/cc) can also be found around 12:00 hrs, which could be the result of more dilution due to the expanded boundary layer [30] and associated high wind speed at noon (> 3.1 m/s at 12:00-14:00 hrs). Interestingly, the dip in the total volume concentration around noon time is consistent with the mass concentration trend in both hourly $PM_{2.5}$ and PM_{10} pattern in **Fig. S1**.

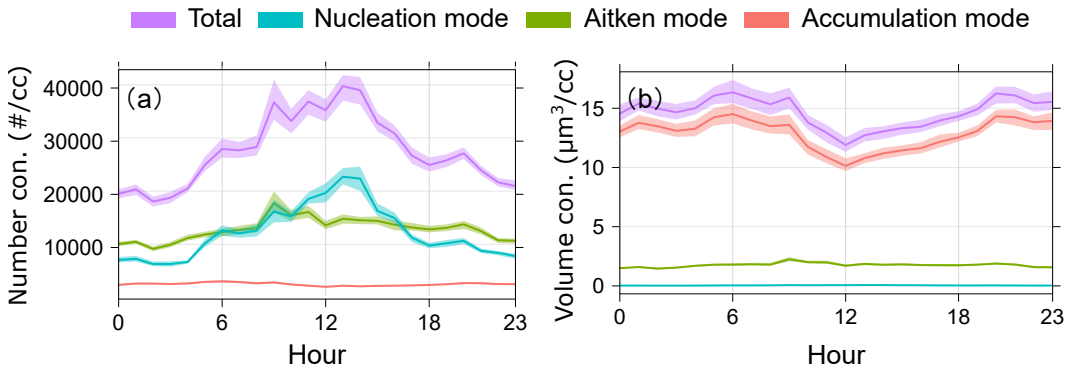

Figure 4: *Hourly number (a) and volume (b) concentration under different modes: nucleation mode (Dp<30 nm), Aitken mode (30<Dp<100 nm) and accumulation mode (100<Dp<1000 nm). The shaded area represents the 95% confidence interval.*

3.2 Source apportionment on PNSD

From the above analysis, the PNSD in Singapore is mainly composed of ultrafine particles at nucleation mode and Aitken mode. The diurnal and nocturnal pattern of the particle

concentration shows correlation with traffic rush hours and meteorological variations. In order to better understand the key processes and possible sources of the airborne PM emissions, a source apportionment study was performed in this section on particle number concentration and size distribution.

Here, all data obtained from DMS were averaged to 5 min resolution to minimize undesirable noise and retain high time resolution synchronizing with the meteorological data [30]. As a result, 7174 samples of PNSD each with 38 size bins are prepared as the input file for PMF analysis. Each bin is evenly logarithmically spaced, where the logarithmic difference between each size bin is 1/16. Total particle number concentration of all samples was used in the analysis as an indicator and assigned in the software. Due to the low signal-noise ratio, the first three size bins (< 6.5 nm) were assigned an uncertainty of 300%, being considered as weak variables [34].

In order to determine the best number of factors, the model was operated with 3 to 7 factors in this study. The 5-factor solution was selected as the most physically plausible case, and the sum of weighted least squares Q is closer to the expected value calculated as suggested by [36]. For solutions having a number of factors smaller than 5, Qs are considerably larger than the expected values which is a result of unresolved sources. In those cases, a large number of size bins show large scaled residuals and a poor fitting of total number concentration ($R^2 < 0.9$). For solutions having a number of factors larger than 5, Qs are lower than the expected value, and the spurious factors appear without distinct physical meaning. These spurious factors only exhibit a negligible contribution to the total particle number concentration. In addition, the 5-factor solution is robust through the in-built error estimation and no significant rotational ambiguities were found. A summary of key parameters in the process is presented in **Table. S1**.

The results of PMF are presented in Fig. 5. Each row corresponds to a factor. The left column are particle size profiles in number (solid line) and volume concentration (dash line); the middle column are temporal patterns of factor contributions (the shaded area represents the 95% confidence interval); the right column are the results of bivariate CPF analysis, where both wind speed (ws) and wind direction (wd) data were used to plot the CPF probability. For direct comparison between different factors, all factor contributions were normalized and the axis limits were set at fixed values for most cases. A summary of the factors with related processes and potential sources is shown in Table 1.

Factor 1 is the largest contributor to total number concentration, accounting for 34.6%. It is also the third largest contributor to total volume concentration. From the size distribution pattern, the mode size for the major sharp peak in number concentration is at 42-49 nm in the Aitken mode, with minor peak at 6-7 nm. In volume concentration, there are two peaks; the major peak is at 100-116 nm and the minor one is at 487-562 nm. From the temporal trend in Fig. 5, the factor is prominent in the morning (8:00-11:00 hrs) and then remains at a high level (above 1.0) until 21:00 hrs. The peak at morning traffic rush hours in temporal trend implies that the factor could be related to traffic emissions. Aged traffic-related particles are reported to be around 50 nm in big cities, and generally accounts for a major part in total number concentration (>30%) [33, 41, 42]. Besides, considering the CPF results, factor 1 can be associated with the winds mainly from southwest, where industry park (petrochemical refinery) and harbor (shipping) exist. Similar size distribution patterns are also reported to represent industrial activities in Ostrava (mode size at 45 nm),

Table 1: *Summary of the factors with related processes and potential sources.*

	Contribution[1]	Size range	Major processes	Potential sources
Factor 1	34.6%	Aitken	Primary emissions	Aged traffic, industry
Factor 2	13.0%	Nucleation	Atmospheric photochemical reactions	O_3-related precursors
Factor 3	30.5%	Nucleation	Combustion-related	Fresh traffic, industry
Factor 4	4.2%	Accumulation	Mixture, urban background	Marine aerosols, secondary aerosols
Factor 5	17.7%	Aitken	Combustion-related	Stationary combustion, cooking

[1] Contribution to particle total number concentration.

Kuwait City (mode size at 42 nm) and Rochester (mode size at 40-50 nm) [30, 34, 43]. In the studied area, factor 1 could be a mixture of both aged traffic and industrial emissions.

Factor 2 has a contribution of 13.0% to total number concentration, and a negligible contribution to total volume concentration. From the size distribution pattern, the mode size for the sharp peak in number concentration is at 10-12 nm, within the nucleation mode. From the temporal pattern, the factor has a very high normalized contribution (>1.5) from 12:00-15:00 hrs and remains weak through the rest of the day. Based on previous analysis of particle diurnal pattern, factor 2 is strongly related to the short-lived nucleation events that occur at early afternoon, mainly caused by photochemical reactions in the atmosphere. From the CPF results, it shows association with a wide range of wind directions from north, west and south. Consistent temporal trend in O_3 concentration (shown in **Fig. S1**) demonstrates prominent photooxidation of volatile organic compounds at early afternoon. Hence, factor 2 can be attributed to nucleation events mainly driven by atmospheric photochemical reactions. Such factor is rarely reported in literature and the peak particle size of factor 2 is smaller than the O_3-rich secondary aerosol reported in other cities at about 50 nm [42, 43].

Factor 3 is the second largest contributor to total number concentration (30.5%), while its contribution to volume concentration is almost negligible. From the size distribution pattern, the mode size for the single sharp peak in number concentration is at 15-20 nm, within the nucleation mode. From the temporal pattern, the factor is prominent at multiple time periods, including early morning (6:00 hrs), morning traffic hour (9:00-10:00 hrs), early afternoon (12:00-14:00 hrs) and late afternoon traffic hour (19:00-20:00 hrs). Compared to factor 2, it has a broader temporal pattern and correlates well with both morning traffic and afternoon rush hours. Based on above facts, factor 3 can be linked with the traffic and combustion. The precursor gases from possible sources like fresh traffic and industry form these particles through nucleation. Several studies have also reported similar nucleation mode particles from fresh road traffic and industry emissions [30, 34, 41, 43]. From the CPF results, it shows an association with the winds at lower speed from west and at higher speed (> 4 m/s) from north, which may correspond to fresh traffic emissions at nearby expressways and possible precursors transported from north.

Factor 4 is the largest contributor to total volume concentration but plays a small part

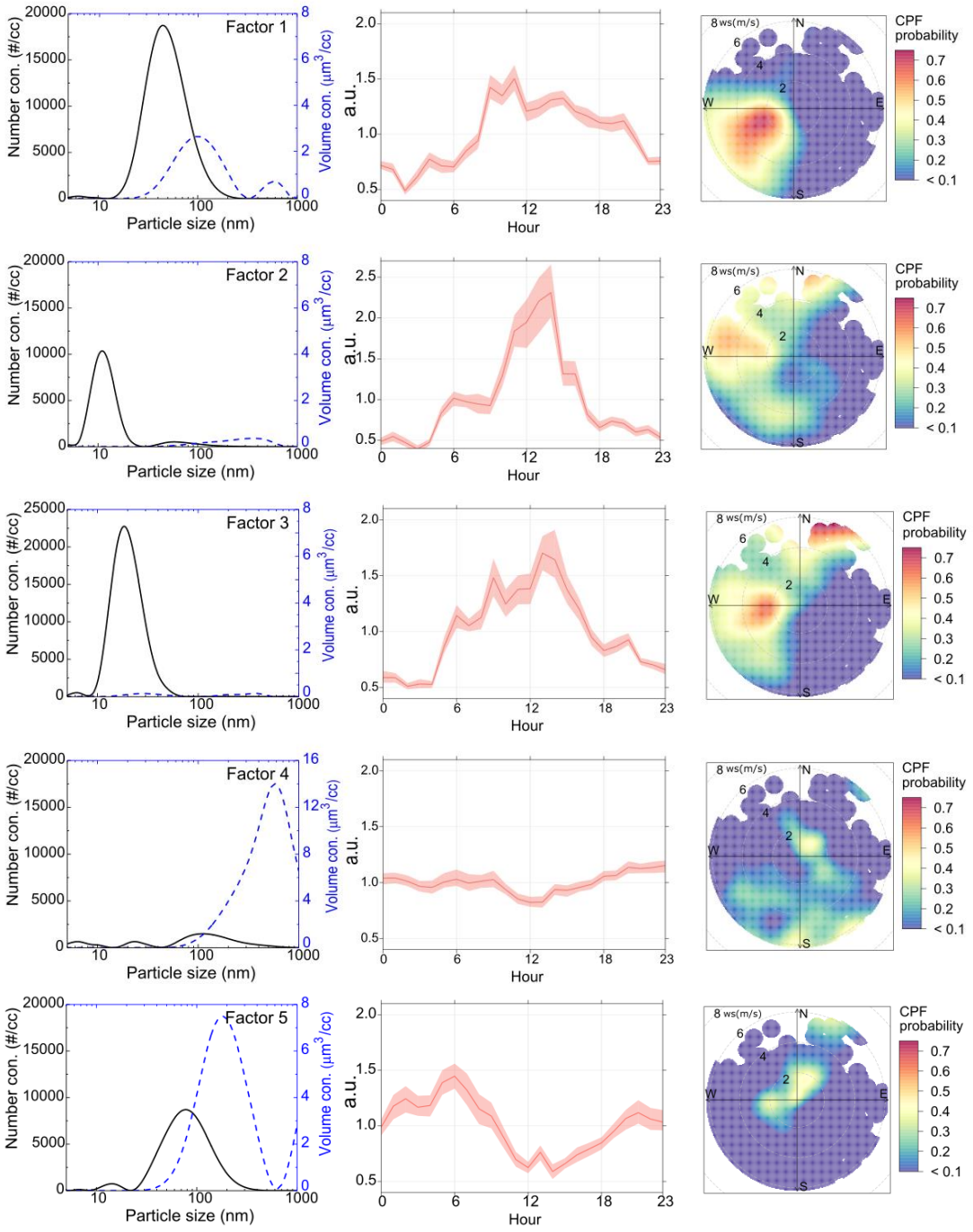

Figure 5: *Left: Factor profiles in number (solid line) and volume concentration (dash line). Middle: temporal pattern of factor contributions, the shaded area represents the 95% confidence interval. Right: the results of bivariate CPF analysis for each factor.*

in number concentration (4.2%). From the size distribution pattern, the mode size for the major peak in number concentration is at 100-116 nm, within accumulation mode; and minor peaks exist at 6-7 nm and 21-27 nm. In volume concentration, the mode size for the single peak is at 487-562 nm. More than 70% of accumulation mode particles at 300-1000 nm are attributed to factor 4. From the temporal pattern, the factor remains relatively invariable during the day and night, and reaches the lowest level at the noon, which could be due to the highest planetary boundary layer that substantially depends on vertical temperature profile. Similar temporal trends can be found for PM_{10} and $PM_{2.5}$ (shown in **Fig. S1**). In terms of size distribution and temporal pattern, factor 4 could be the mixture of transported particles from exhaust emissions and secondary aerosols, which serve as the urban background in the studied area [30, 34]. In CPF analysis, it associates with wind from the south at high speed (> 4 m/s), where sea and harbor exist. Possible source of factor 4 could involve sea salt particles in accumulation mode. Typical mode size of sea salt particles is reported as 100 nm from film droplets (break-up droplets) evaporation [44], and above 1000 nm from the evaporation of complete droplets [27], which is beyond the measurement range of this study.

Factor 5 is the third largest contributor to total number concentration, and accounts for 17.7%. It is also the second largest contributor to the total volume concentration. From the size distribution pattern, the mode size for the major peak in number concentration is at 75-87 nm, with Aitken mode; and a minor peak exists at about 15 nm. In volume concentration, the peak is at around 154-178 nm and from the profile there could be a second peak coarse particles larger than 1000 nm which is beyond the measurement limit in this study. From the temporal pattern, the factor has peaks at the early morning between 4:00-8:00 hrs, and is prominent at nighttime, before 8:00 and after 20:00 hrs, which is consistent with the temporal trend in NO_2 and CO concentration (shown in **Fig. S1**). This factor could be related to the primary emission of fuel combustion considering the typical particle size distribution, as the mode size is reported at 70-80 nm for stationary combustion in Augsburg [45] and at 100 nm for fuel combustion in Beijing [33]. In CPF analysis, it shows an association with low speed winds from wide range of directions and winds from northeast at high wind speeds (> 4 m/s), which may introduce cooking emissions at nearby residential areas and stationary combustion emissions from cross-border sources.

Based on above analysis, five factors were resolved and identified as aged traffic and industrial emissions (34.6%), atmospheric photochemical reactions (13.0%), fresh traffic emissions (30.5%), urban background (4.2%) and fuel combustion (17.7%). Among the five factors, two factors (atmospheric photochemical reactions and fresh traffic emissions) are closely related to the nucleation events frequently found in the morning and early afternoon, which together account for 43.5% of total number concentration of particles between 5-1000 nm. This percentage is higher than that in other big cities with available monitoring data [33, 41, 42]. In terms of Aitken mode particles in the studied area, they show characteristics of aged traffic, industrial emissions and fuel combustion. For accumulation mode particles, marine aerosols (sea salt) and secondary aerosols are the major contributors present in the urban background, which can be important components of mass concentration of PM_{10} and $PM_{2.5}$. Notably, from the CPF results, some cross-border emitters in the northeast are likely to be significant pollution sources at high wind speeds. Future measurements and chemical analyses of multi-pollutants are recom-

mended to verify and elucidate potential source characteristics and related atmospheric processes.

4 Conclusions

In this study, particle number concentration and size distribution in the size range of 5-1000 nm were measured during the southwest monsoon season in 2017 in Singapore. PMF using particle number concentration and size distribution data was performed for the first time in the region. Results of this investigation can be considered as a baseline for Singapore airborne PM emissions, as the measurements comprise a season without major transboundary biomass smoke, together with frequent rain scavenging. Furthermore, the diurnal and nocturnal pattern and source apportionment of PM spectra could be a reference for future studies in Southeast Asia and other tropical large cities.

Particles in the nucleation mode are the largest contributor to the total number concentration in Singapore. Nucleation events were found prominent in the diurnal pattern of PM spectra because of the abundant radiation. Two types of nucleation process were observed: 1) In the morning and evening rush hours associating with traffic emissions; 2) At early afternoon from 12:00 to 15:00 hrs attributing to gas-particle conversion through atmospheric photochemical reactions.

Five major sources were identified with PMF: aged traffic and industrial emissions, atmospheric photochemical reactions, fresh traffic emissions, urban background and fuel combustion. The airborne PM emissions in tropical urban environment are found to have 43.5% of particles originated from nucleation-related processes, i.e., atmospheric photochemical reactions and fresh traffic emissions, which is higher than the available monitoring data in other big cities. Among them, O_3-related atmospheric photochemical reactions with peak size at 10-12 nm is a unique factor prominent in early afternoon.

5 Acknowledgments

This project was funded by the National Research Foundation (NRF), Prime Minister's Office, Singapore under its Campus for Research Excellence and Technological Enterprise (CREATE) programme. The authors thank geography weather station in National University of Singapore (NUS) for the meteorological data.

References

[1] Nick Watts, Markus Amann, Sonja Ayeb-Karlsson, Kristine Belesova, Timothy Bouley, Maxwell Boykoff, Peter Byass, Wenjia Cai, Diarmid Campbell-Lendrum, and Jonathan Chambers. The Lancet countdown on health and climate change: from 25 years of inaction to a global transformation for public health. *The Lancet*, 6736 (17), 2017. doi:10.1016/S0140-6736(17)32464-9.

[2] Rudy Sinharay, Jicheng Gong, Benjamin Barratt, Pamela Ohman-Strickland, Sabine Ernst, Frank Kelly, Junfeng Jim Zhang, Peter Collins, Paul Cullinan, and Kian Fan Chung. Respiratory and cardiovascular responses to walking down a traffic-polluted road compared with walking in a traffic-free area in participants aged 60 years and older with chronic lung or heart disease and age-matched healthy controls: a randomised, crossover study. *The Lancet*, 6736(17):1–11, 2017. doi:10.1016/S0140-6736(17)32643-0.

[3] James S Brown, Terry Gordon, Owen Price, and Bahman Asgharian. Thoracic and respirable particle definitions for human health risk assessment. *Particle and Fibre Toxicology*, 10(1):12, 2013. doi:10.1186/1743-8977-10-12.

[4] Angela Ibald-Mulli, H-Erich Wichmann, Wolfgang Kreyling, and Annette Peters. Epidemiological evidence on health effects of ultrafine particles. *Journal of Aerosol Medicine*, 15(2):189–201, 2002. doi:10.1089/089426802320282310.

[5] Prashant Kumar, Alan Robins, Sotiris Vardoulakis, and Rex Britter. A review of the characteristics of nanoparticles in the urban atmosphere and the prospects for developing regulatory controls. *Atmospheric Environment*, 44(39):5035–5052, 2010. doi:10.1016/j.atmosenv.2010.08.016.

[6] Butchaiah Gadde, Sébastien Bonnet, Christoph Menke, and Savitri Garivait. Air pollutant emissions from rice straw open field burning in India, Thailand and the Philippines. *Environmental Pollution*, 157(5):1554–1558, 2009. doi:10.1016/j.envpol.2009.01.004.

[7] Doreena Dominick, Mohd Talib Latif, Liew Juneng, Md Firoz Khan, Norhaniza Amil, Mohammed Iqbal Mead, Mohd Shahrul Mohd Nadzir, Phang Siew Moi, Azizan Abu Samah, and Matthew J Ashfold. Characterisation of particle mass and number concentration on the east coast of the Malaysian Peninsula during the northeast monsoon. *Atmospheric Environment*, 117:187–199, 2015. doi:10.1016/j.atmosenv.2015.07.018.

[8] Shirani Seneviratne, Lakmali Handagiripathira, Sisara Sanjeevani, Dulanjalee Madusha, Vajira Ariyaratna Ariyaratna Waduge, Thilaka Attanayake, Deepthi Bandara, and Philip K Hopke. Identification of sources of fine particulate matter in Kandy, Sri Lanka. *Aerosol and Air Quality Research*, 17(2):476–484, 2017.

[9] R Balasubramanian, W-B Qian, S Decesari, MC Facchini, and S Fuzzi. Comprehensive characterization of PM2.5 aerosols in Singapore. *Journal of Geophysical Research: Atmospheres*, 108(D16), 2003. doi:10.1029/2002JD002517.

[10] Santo V Salinas, Boon Ning Chew, Jukka Miettinen, James R Campbell, Ellsworth J Welton, Jeffrey S Reid, E Yu Liya, and Soo Chin Liew. Physical and optical characteristics of the October 2010 haze event over Singapore: A photometric and lidar analysis. *Atmospheric Research*, 122:555–570, 2013. doi:10.1016/j.atmosres.2012.05.021.

[11] Hsiang-He Lee, Rotem Z Bar-Or, and Chien Wang. Biomass burning aerosols and the low-visibility events in Southeast Asia. *Atmospheric Chemistry and Physics*, 17 (2):965–980, 2017. doi:10.5194/acp-17-965-2017.

[12] Ailu Chen, Qingliang Cao, Jin Zhou, Bin Yang, Victor W-C Chang, and William W Nazaroff. Indoor and outdoor particles in an air-conditioned building during and after the 2013 haze in Singapore. *Building and Environment*, 99:73–81, 2016. doi:10.1016/j.buildenv.2016.01.002.

[13] Erik Velasco and Sok Huang Tan. Particles exposure while sitting at bus stops of hot and humid Singapore. *Atmospheric Environment*, 142:251–263, 2016. doi:10.1016/j.atmosenv.2016.07.054.

[14] Sok Huang Tan, Matthias Roth, and Erik Velasco. Particle exposure and inhaled dose during commuting in Singapore. *Atmospheric Environment*, 170:245–258, 2017. doi:10.1016/j.atmosenv.2017.09.056.

[15] Zhi-Hui Zhang, Andrey Khlystov, Leslie K Norford, Zhen-Kang Tan, and Rajasekhar Balasubramanian. Characterization of traffic-related ambient fine particulate matter (PM2.5) in an Asian city: Environmental and health implications. *Atmospheric Environment*, 161:132–143, 2017. doi:10.1016/j.atmosenv.2017.04.040.

[16] M Brines, Manuel Dall'Osto, DCS Beddows, RM Harrison, F Gómez-Moreno, L Núñez, B Artíñano, F Costabile, GP Gobbi, F Salimi, et al. Traffic and nucleation events as main sources of ultrafine particles in high-insolation developed world cities. *Atmospheric Chemistry and Physics*, 15(10):5929–5945, 2015. doi:10.5194/acp-15-5929-2015.

[17] Raghu Betha, Dominick V Spracklen, and Rajasekhar Balasubramanian. Observations of new aerosol particle formation in a tropical urban atmosphere. *Atmospheric Environment*, 71:340–351, 2013. doi:10.1016/j.atmosenv.2013.01.049.

[18] VP Kanawade, Sachchida N Tripathi, Devendraa Siingh, Alok S Gautam, Atul K Srivastava, Adarsh K Kamra, Vijay K Soni, and Virendra Sethi. Observations of new particle formation at two distinct indian subcontinental urban locations. *Atmospheric Environment*, 96:370–379, 2014. doi:10.1016/j.atmosenv.2014.08.001.

[19] Cheol-Heon Jeong, Philip K Hopke, David Chalupa, and Mark Utell. Characteristics of nucleation and growth events of ultrafine particles measured in

Rochester, NY. *Environmental Science & Technology*, 38(7):1933–1940, 2004. doi:10.1021/es034811p.

[20] Pentti Paatero and Unto Tapper. Analysis of different modes of factor analysis as least squares fit problems. *Chemometrics and Intelligent Laboratory Systems*, 18 (2):183–194, 1993. doi:10.1016/0169-7439(93)80055-M.

[21] Pentti Paatero. Least squares formulation of robust non-negative factor analysis. *Chemometrics and Intelligent Laboratory Systems*, 37(1):23–35, 1997. doi:10.1016/S0169-7439(96)00044-5.

[22] Yu Song, Yuanhang Zhang, Shaodong Xie, Limin Zeng, Mei Zheng, Lynn G Salmon, Min Shao, and Sjaak Slanina. Source apportionment of PM2.5 in Beijing by positive matrix factorization. *Atmospheric Environment*, 40(8):1526–1537, 2006. doi:10.1016/j.atmosenv.2005.10.039.

[23] D Cesari, A Genga, P Ielpo, M Siciliano, G Mascolo, FM Grasso, and D Contini. Source apportionment of PM2.5 in the harbour-industrial area of Brindisi (Italy): Identification and estimation of the contribution of in-port ship emissions. *Science of the Total Environment*, 497:392–400, 2014. doi:10.1016/j.scitotenv.2014.08.007.

[24] Philip K Hopke. Review of receptor modeling methods for source apportionment. *Journal of the Air & Waste Management Association*, 66(3):237–259, 2016. doi:10.1080/10962247.2016.1140693.

[25] D Ogulei, PK Hopke, and LA Wallace. Analysis of indoor particle size distributions in an occupied townhouse using positive matrix factorization. *Indoor Air*, 16(3): 204–215, 2006. doi:10.1111/j.1600-0668.2006.00418.x.

[26] David Ogulei, Philip K Hopke, Liming Zhou, J Patrick Pancras, Narayanan Nair, and John M Ondov. Source apportionment of Baltimore aerosol from combined size distribution and chemical composition data. *Atmospheric Environment*, 40:396–410, 2006. doi:10.1016/j.atmosenv.2005.11.075.

[27] Tuan V Vu, Juana Maria Delgado-Saborit, and Roy M Harrison. Particle number size distributions from seven major sources and implications for source apportionment studies. *Atmospheric Environment*, 122:114–132, 2015. doi:10.1016/j.atmosenv.2015.09.027.

[28] Maria L Botero, Sebastian Mosbach, and Markus Kraft. Sooting tendency of paraffin components of diesel and gasoline in diffusion flames. *Fuel*, 126:8–15, 2014. doi:10.1016/j.fuel.2014.02.005.

[29] Prashant Kumar, Paul Fennell, David Langley, and Rex Britter. Pseudo-simultaneous measurements for the vertical variation of coarse, fine and ultrafine particles in an urban street canyon. *Atmospheric Environment*, 42(18):4304–4319, 2008. doi:10.1016/j.atmosenv.2008.01.010.

[30] Abdullah N Al-Dabbous and Prashant Kumar. Source apportionment of airborne nanoparticles in a Middle Eastern city using positive matrix factorization. *Environmental Science: Processes & Impacts*, 17(4):802–812, 2015. doi:doi.org/10.1039/C5EM00027K.

[31] David C Carslaw and Karl Ropkins. Openair - an R package for air quality data analysis. *Environmental Modelling & Software*, 27:52–61, 2012. doi:10.1016/j.envsoft.2011.09.008.

[32] GA Norris, R Duvall, SG Brown, and S Bai. EPA Positive Matrix Factorization (PMF) 5.0 fundamentals and user guide prepared for the US Environmental Protection Agency Office of Research and Development, Washington, DC. *U.S. EPA*, 2014.

[33] ZB Wang, M Hu, ZJ Wu, DL Yue, LY He, XF Huang, XG Liu, and A Wiedensohler. Long-term measurements of particle number size distributions and the relationships with air mass history and source apportionment in the summer of Beijing. *Atmospheric Chemistry and Physics*, 13(20):10159–10170, 2013. doi:10.5194/acp-13-10159-2013.

[34] Cecilia Leoni, Petra Pokorná, Jan Hovorka, Mauro Masiol, Jan Topinka, Yongjing Zhao, Kamil Krumal, Steven Cliff, Pavel Mikuska, and Philip K Hopke. Source apportionment of aerosol particles at a european air pollution hot spot using particle number size distributions and chemical composition. *Environmental Pollution*, 234: 145–154, 2018. doi:10.1016/j.envpol.2017.10.097.

[35] Mauro Masiol, Roy M Harrison, Tuan V Vu, and David CS Beddows. Sources of sub-micrometre particles near a major international airport. *Atmospheric Chemistry and Physics*, 17(20):12379, 2017. doi:10.5194/acp-17-12379-2017.

[36] Steven G Brown, Shelly Eberly, Pentti Paatero, and Gary A Norris. Methods for estimating uncertainty in PMF solutions: Examples with ambient air and water quality data and guidance on reporting PMF results. *Science of the Total Environment*, 518: 626–635, 2015. doi:10.1016/j.scitotenv.2015.01.022.

[37] Iratxe Uria-Tellaetxe and David C Carslaw. Conditional bivariate probability function for source identification. *Environmental modelling & software*, 59:1–9, 2014. doi:10.1016/j.envsoft.2014.05.002.

[38] M Kulmala, V-M Kerminen, T Petäjä, AJ Ding, and L Wang. Atmospheric gas-to-particle conversion: why NPF events are observed in megacities? *Faraday Discussions*, 200:271–288, 2017. doi:10.1039/C6FD00257A.

[39] Charles O Stanier, Andrey Y Khlystov, and Spyros N Pandis. Nucleation events during the Pittsburgh air quality study: description and relation to key meteorological, gas phase, and aerosol parameters special issue of aerosol science and technology on findings from the fine particulate matter supersites program. *Aerosol Science and Technology*, 38(S1):253–264, 2004. doi:10.1080/02786820390229570.

[40] Joe Cheung, Lidia Morawska, and Zoran Ristovski. Observation of new particle formation in subtropical urban environment. *Atmospheric Chemistry and Physics (ACP) & Discussions (ACPD)*, 11:3823–3833, 2011. doi:10.5194/acp-11-3823-2011.

[41] Roy M Harrison, David CS Beddows, and Manuel Dall'Osto. PMF analysis of wide-range particle size spectra collected on a major highway. *Environmental Science and Technology*, 45(13):5522–5528, 2011. doi:10.1021/es2006622.

[42] M Masiol, PK Hopke, HD Felton, BP Frank, OV Rattigan, MJ Wurth, and GH LaDuke. Source apportionment of PM2.5 chemically speciated mass and particle number concentrations in New York City. *Atmospheric Environment*, 148:215–229, 2017. doi:10.1016/j.atmosenv.2016.10.044.

[43] David Ogulei, Philip K Hopke, David C Chalupa, and Mark J Utell. Modeling source contributions to submicron particle number concentrations measured in Rochester, New York. *Aerosol Science and Technology*, 41(2):179–201, 2007. doi:10.1080/02786820601116012.

[44] E Monica Mårtensson, Peter Tunved, Hannele Korhonen, and E Douglas Nilsson. The role of sea-salt emissions in controlling the marine Aitken and accumulation mode aerosol: a model study. *Tellus B*, 62(4):259–279, 2010. doi:10.1111/j.1600-0889.2010.00465.x.

[45] Jianwei Gu, Mike Pitz, Jürgen Schnelle-Kreis, Jürgen Diemer, Armin Reller, Ralf Zimmermann, Jens Soentgen, Matthias Stoelzel, H-Erich Wichmann, and Annette Peters. Source apportionment of ambient particles: comparison of positive matrix factorization analysis applied to particle size distribution and chemical composition data. *Atmospheric Environment*, 45(10):1849–1857, 2011. doi:10.1016/j.atmosenv.2011.01.009.

6 Supporting Material

1. Table S1. Key parameters in PMF solutions with different factor numbers.
2. Figure S1. Temporal trend in mass concentrations of PM_{10}, $PM_{2.5}$, O_3, NO_2, SO_2 and CO during the measurement campaign (mg/m^3 for CO and μg/m^3 for the rest). PM_{10}, $PM_{2.5}$ and SO_2 are presented by 24-hour mean value. O_3 and SO_2 are presented by 8-hour mean value. NO_2 is presented by 1-hour mean value. Data are provided by NEA from data.gov.sg/group/environment.

Table S1: *Key parameters in PMF solutions with different factor numbers.*

	3 factors	**4 factors**	**5 factors**	**6 factors**	**7 factors**
Qexpected (Qe)	229463	222254	215045	207836	200627
Qrobust (Qr)	688816	417538	224770	142128	88535
Qr/Qe	3.00	1.88	1.05	0.68	0.44
R^2 (total con.)	0.795	0.827	0.943	0.957	0.965
Slope (total con.)	0.791	0.809	0.922	0.933	0.941
BS (<100%)	-	2	0	1	-
DISP	-	0	0	0	-
BS-DISP	-	0	0	0	-

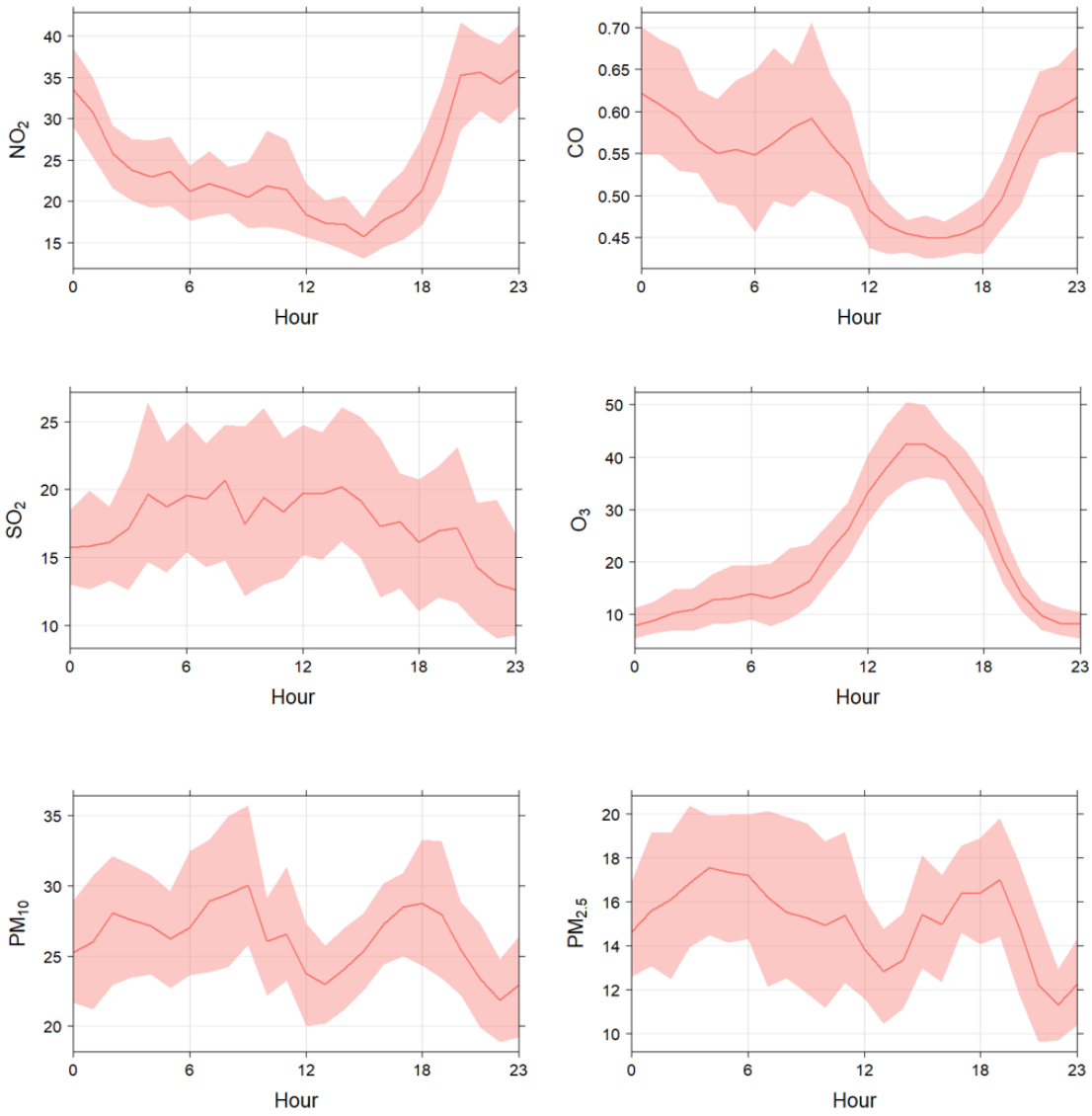

Figure S1: *Temporal trend in mass concentrations of PM_{10}, $PM_{2.5}$, O_3, NO_2, SO_2 and CO during the measurement campaign ((mg/m^3 for CO and µg/m^3 for the rest). The shaded area represents the 95% confidence interval.*